

# Spatially resolved wettability measurements using nmr wettability index

M. J. Dick<sup>1,\*</sup>, D. Veselinovic<sup>1</sup>, and D. Green<sup>1</sup>

<sup>1</sup>Green Imaging Technologies, Fredericton, NB, Canada

**Abstract.** Wettability is a crucial petrophysical parameter for determining accurate production rates in oil and gas reservoirs. However, industry standard wettability measurements (Amott Test and USBM) are expensive and time consuming. It is known that NMR response varies as a function of wettability change in rock core plug samples. This information was used to develop an NMR wettability index (NWI) based on T<sub>2</sub> distributions. This NWI is capable of measuring changes in wettability as a function of oil/water saturations unlike traditional methods which are based on measurements at Swi and Sor only. In addition, these oil/water saturations are determined without the aid of any special oil or brine, such as D2O. This allows the NMR method to nondestructively monitor changes in wettability in real time (i.e. during a flooding experiment or an aging procedure). In this work, we have coupled this T<sub>2</sub>-based NWI to spatially resolved T<sub>2</sub> NMR measurements to monitor changes in wettability and saturation along rock core plugs. In order to derive an NMR wettability index, NMR T<sub>2</sub> spectra of 100% brine saturated, 100% oil saturated, bulk oil and bulk brine are needed. These spectra are then mixed to give a predicted T<sub>2</sub> spectrum which is compared (via a least squares fit) to a T<sub>2</sub> spectrum recorded from a sample partially saturated with both water and oil and whose wettability is to be determined. For initial testing, three sandstone samples were employed along with 2% KCl brine and dodecane. To achieve sample states of mixed wettability, 100% brine saturated samples had dodecane pushed into them via centrifugation. Centrifugation at different speeds resulted in samples of varying bulk and spatial wettabilities from which NWI parameters and oil/water saturations were determined. The bulk wettabilities were compared to measurements done using the standard Amott test and oil/water saturations were confirmed by repeating experiments using NMR invisible D2O.

## 1 Introduction

Wettability can be thought of as the tendency of a surface to maintain contact with a fluid. Inside the pores of a rock, this tendency of the surface can either favor water or oil adherence to the surface of the pores. Quantitatively this can be defined as [1],

$$I_w = \frac{A_w - A_o}{A_w + A_o} \quad (1)$$

where A<sub>w</sub> is the surface area wetted by water and A<sub>o</sub> is the surface area wetted by oil. From the equation it is obvious that if more surface area is wetted by water then I<sub>w</sub> = 1 to 0. Conversely, if there is more surface area wetted by oil then I<sub>w</sub> = 0 to -1.

NMR is well suited to measure wettability because surface area wetted by either water or oil can be derived from the transverse relaxation time, T<sub>2</sub>. Quantitatively, T<sub>2</sub> relaxation times of oil and water inside a pore network are defined as follows.

$$\frac{1}{T_{2w}} = \frac{1}{T_{2bulkw}} + \rho_w \frac{A_w}{V_w} \frac{1}{T_{2o}} = \frac{1}{T_{2bulko}} + \rho_o \frac{A_o}{V_o} \quad (2)$$

Where T<sub>2w</sub> is the relaxation time for water in the pores, T<sub>2bulkw</sub> is the relaxation time of bulk water, V<sub>w</sub> is the pore volume occupied by water and ρ<sub>w</sub> is the surface relaxivity parameter for water. T<sub>2o</sub> is the relaxation time for oil in the pores, T<sub>2bulko</sub> is the relaxation time of bulk oil, V<sub>o</sub> is the pore volume occupied by oil and ρ<sub>o</sub> is the surface relaxivity parameter for oil.

There have been several attempts to exploit the ability of NMR to measure the surface areas occupied by oil and water and hence derive an NMR based wettability parameter [1-5]. We have chosen to employ the method developed by Looyestijn et.al. [6,7] because it allows wettability to be predicted during a flood as a function of water saturation. In this method, the observed T<sub>2</sub> distribution from a sample of mixed saturation (i.e. partially saturated with both oil and water) is recorded. This T<sub>2</sub> distribution is then compared via a least-squares fit to a simulated distribution comprised of contributions from measured T<sub>2</sub> distributions of 100% brine saturated, 100% oil saturated, bulk oil and bulk brine. The various

\* corresponding author: [mjdick@greenimaging.com](mailto:mjdick@greenimaging.com)

distributions are combined using mixing functions based on the assumption that at any given concentration the smaller pores have a lower oil saturation and are thus more water wet [6]. This assumption is a limitation of the method and may not be valid for all rocks (i.e. samples taken after water based mud invasion where water can be present even in the biggest pores). The result of the fit is both the wettability and the relative oil/water saturation of the rock.

We have furthered the work of Looyestijn by combining his method of determining wettability from  $T_2$  distributions to spatial- $T_2$  measurements. Spatial- $T_2$  distributions measure  $T_2$  distributions as a function of position in the rock. This has allowed us to track both wettability and saturation as a function of position in the rock. This new measurement opens a whole batch of new wettability-based experiments, including the ability to track wettability during a flooding experiment, as well as, measuring wettability at different saturation levels during one measurement from one sample.

## 2 Experimental

Three sandstone samples were chosen for this wettability study. The characteristic information for each rock is shown in Table 1. 2% KCl Brine and dodecane were employed as the saturating fluids in this wettability study. Dodecane was chosen as it has a simple  $T_2$  distribution as compared to many crude oils. The disadvantage of choosing dodecane is that when coupled with brine it may not contain the necessary constituents (i.e. divalent ions) to bring about a wettability change.  $T_2$  distributions for each bulk fluid ( $S_{w-bulk}$  and  $S_{o-bulk}$ ) were recorded using the NMR parameters outlined in the second column of Table 2.

**Table 1:** Properties of core plug studied

Name	96S	109S	62A
Core Diameter (cm)	3.81	3.81	3.81
Core Length (cm)	4.91	4.81	5.38
Dry Core Mass (g)	117.67	119.36	140.93
Pore Volume (mL)	9.079	8.461	8.080
Bulk Volume (mL)	55.97	54.838	61.337
Porosity (p.u.)	0.1622	0.1543	0.1317

To properly derive the wettabilities, the bulk  $T_2$  distributions of water and dodecane are combined with the  $T_2$  distributions of the three sandstone samples measured in the following states, 100% saturated with brine ( $S_{w-100\%}$ ), 100% saturated with dodecane ( $S_{o-100\%}$ ) and a mixed

saturation state ( $S_{mix}$ ). To achieve each of these states on each sample the following procedure was followed.

1. Each sample, initially in a clean and dry state, was first saturated with brine via vacuum saturation.
2.  $T_2$  and spatial- $T_2$  distributions were then recorded for the 100% brine saturated state ( $S_{w-100\%}$ ). The NMR parameters employed for each of these measurements are outlined in columns 3 and 5 of Table 2.
3. The  $S_{w-100\%}$  samples were centrifuged for approximately 12 hours surrounded by dodecane. This resulted in samples of mixed saturation ( $S_{mix}$ ) and spinning the same samples at different speeds resulted in samples of differing dodecane/brine saturations. Samples 96S and 109S were spun at 700, 800, 3000 and 7500 RPM (78 to 8968 times the force of gravity [8]). Sample 62A was spun at 1200, 3000, and 7500 RPM (229 to 8968 times the force of gravity [8]).
4.  $T_2$  and spatial- $T_2$  distributions were then recorded for each mixed saturation state achieved via centrifugation. NMR parameters for these measurements are again summarized in Table 2.
5. After spinning at 7500 RPM, each sample was dried at 70C for 24-48 hours. The drying removed any excess brine and/or dodecane from the sample. As dodecane and water are volatile, drying the samples was sufficient for returning them to clean and dry state. Since we employed low concentration brine (2% KCl in water), we didn't expect any complications from the salt remaining after drying to have any effect on our wettability determination.
6. The dry rocks were then saturated via pressure saturation at 5000 PSI for 12-24 hours.  $T_2$  and spatial- $T_2$  distributions were then recorded for this 100% dodecane saturated state. NMR parameters for these measurements are again summarized in Table 2.

How all this data is analyzed to yield wettability and saturation of bulk measurements along with spatially resolved wettability and saturations will be outlined in the next section of this paper. All NMR measurements were completed on an Oxford Instruments GeoSpec 2<sup>+</sup>-75 rock core analyzer [9]. Acquisition and processing of the NMR data was achieved via Green Imaging Technologies software [10].

**Table 2:** Acquisition parameters for  $T_2$  and spatial- $T_2$  measurements

NMR Parameter	Bulk Brine/ Dodecane- $T_2$	Sample Saturated Dodecane- $T_2$	Brine/ Dodecane- $T_2$	NMR Parameter	Spatial $T_2$
Recycle delay (ms)	22500	7500		Recycle delay (ms)	7500
Tau ( $\mu$ s)	99	99		Tau ( $\mu$ s)	100
Number of Echoes	75758	25253		Number of Echoes	24993
Filter Width (kHz)	125	125		Filter Width (kHz)	125
$T_2$ Max (ms)	3000	1000		$T_2$ Max (ms)	1000
90° Pulse Length ( $\mu$ s)	11.22	11.22		Resolution	64
180° Pulse Length ( $\mu$ s)	22.50	22.44		Gradient Duration ( $\mu$ s)	300
				Resolution (cm)	7

### 3 Data analysis

Looyestijn [6-7] has already discussed the derivation of his NMR wettability analysis. We will instead only present an overview of how we implemented his wettability analysis in this work. Specifically, how we applied it to give spatially resolved wettability.

As shown in Equations 3 and 4, we employed the same functions derived by Looyestijn [6] to describe the saturation and wettability as a function of pore size.

$$H = \frac{a_1 - a_2}{1 + \left(\frac{r}{r_a}\right)^\alpha} + a_2 \rightarrow \frac{1}{1 + \left(\frac{T_2}{r_a}\right)^\alpha}, \quad (3,4)$$

$$W = \frac{b_1 - b_2}{1 + \left(\frac{r}{r_b}\right)^\beta} + b_2 \rightarrow \frac{1}{1 + \left(\frac{T_2}{r_b}\right)^\beta}$$

H describes the fraction of pores occupied by water and W describes the fraction of pores wetted by water. Following the work of Looyestijn [6] which found these constants to be the same for all rocks, we fixed  $a_1$  and  $b_1 = 1$ ,  $a_2$  and  $b_2$  equal to 0 as well as  $\alpha$  and  $\beta$  equal to 2. We also substituted  $r$  by  $T_2$  as transverse relaxation time is proportional to pore size. The typical form of these equations are plotted as the light blue (H) and pink lines (W) in Figure 1. These functions are like step functions, where for example, all pores to the left of the inflection point of the W function are wetted by water and all the pores to the right of the inflection point of the W function are wetted by dodecane. Conversely all the pores to the left of the inflection point of the H function are occupied by brine and all the pores to the right of the inflection point of the H function are occupied by dodecane. As mentioned earlier, these functions act as mixing functions that combine the 100% oil saturated, 100% brine saturated, bulk brine and bulk dodecane  $T_2$  distributions to give a simulated mixed saturation  $T_2$  distribution which closely agrees with the measured mixed saturation  $T_2$  distribution. How this mixing is carried out will now be explained.

All the wettability analysis was carried out in a Matlab routine which read in the  $T_2$  distributions from GIT systems [10]. It should be noted that all our analysis was

done in the  $T_2$  domain. As mentioned by Looyestijn [6], fitting in the time domain is acceptable and sometimes preferred. However, we chose to fit in the  $T_2$  domain as we found the analysis was faster. The speed of the analysis was important to us, especially for spatial- $T_2$  data which could contain as much as 64 times the amount of data compared with bulk  $T_2$  data. We did however carry out a limited amount of analysis in the time domain to verify that the  $T_2$  analysis was consistent with the time domain analysis.

The first step in the wettability investigation was to read in the  $S_{w-bulk}$ ,  $S_{o-bulk}$ ,  $S_{w-100\%}$ ,  $S_{o-100\%}$  and  $S_{mix}$   $T_2$  distributions into the wettability analysis program. The area under each distribution was then normalized to one saturation unit. Figure 1 shows a plot of each of these normalized  $T_2$  distributions. Next a predicted mixed wettability distribution ( $S_{pred}$ ) is generated according to Equation 5.

$$S_{pred} = WHS_{w-100\%} + (1 - W)(1 - H)S_{o-100\%} + (1 - W)HS_{w-bulk} + W(1 - H)S_{o-bulk} \quad (5)$$

How W and H act as mixing functions is now apparent. By multiplying the step functions by the measured  $T_2$  distributions allows portions of each measured spectrum to be combined to give the predicted mixed wettability distribution. The positions of W and H can be adjusted by varying  $r_a$  and  $r_b$  in Equations 3 and 4 giving different contributions to the predicted distributions from each measured distribution. Specifically, a least-squares fit (varying only  $r_a$  and  $r_b$ ) is carried out to minimize the difference between  $S_{mix}$  and  $S_{pred}$ . The black trace in Figure 1 shows the final predicted  $T_2$  distribution generated from the final H (Figure 1 – light blue trace) and W (Figure 1 – pink trace) functions derived from the least squares fitting. As can be seen the final predicted spectrum agrees quite well with the measured mixed saturation distribution (Figure 1- brown trace). Figure 2 shows the contributions to the final predicted  $T_2$  distribution from the  $S_{w-bulk}$ ,  $S_{o-bulk}$ ,  $S_{w-100\%}$  and  $S_{o-100\%}$  distributions.

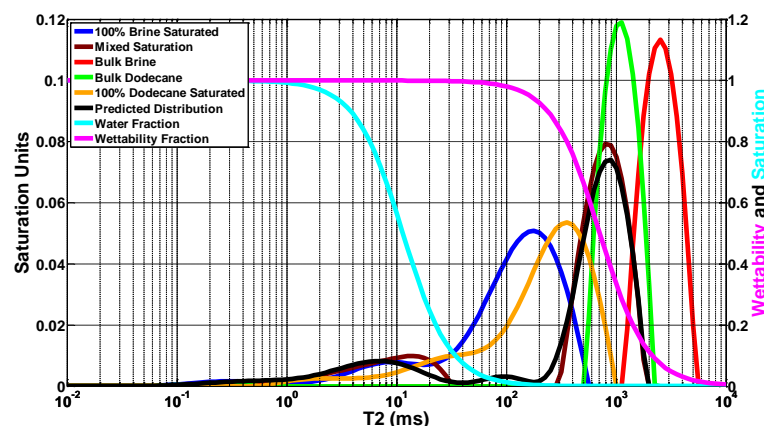


**Fig. 1.** Typical bulk- $T_2$  spectra used for wettability determination (left axis). The water fraction (light blue) and wettability fraction (pink) are also shown (right axis).

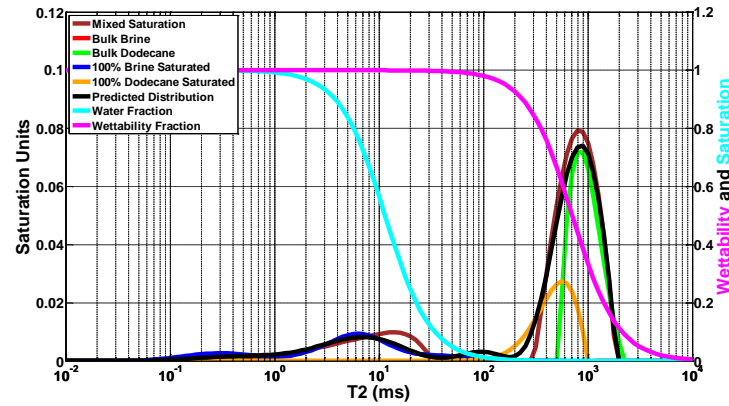


**Fig. 2.** Bulk T<sub>2</sub> spectrum (black) predicted from wettability fitting along with the measured bulk T<sub>2</sub> spectrum (brown) are shown. Also shown are the contributions to the predicted spectrum from the bulk dodecane (green), 100% dodecane saturated (orange) and 100% brine saturated (blue) spectra are also shown. The water fraction (light blue) and wettability fraction (pink) are also shown (right axis).

Once the final H and W functions are known, the saturation and wettability can be quantitatively defined according to Equations 6 and 7. For the data shown in Figure 1 and 2, this corresponds to a  $S_{wett} = 0.13$  and  $I_{wett} = 0.89$ .

$$\text{Water Saturation} = S_{wett} = \sum_{T_2} S_{w-100\%} H \quad (6)$$

$$\text{Wettability} = I_{wett} = 2 \sum_{T_2} S_{w-100\%} W - 1 \quad (7)$$

The above explanation of the wettability analysis was for bulk T<sub>2</sub> distributions but applies also to the spatial-T<sub>2</sub> wettability analysis. The spatial-T<sub>2</sub> data was analyzed for wettability as follows

1. Read in the  $S_{w-bulk}$ ,  $S_{o-bulk}$ , along with the first T<sub>2</sub> slice from the  $S_{w-100\%}$ ,  $S_{o-100\%}$  and  $S_{mix}$  spatial-T<sub>2</sub> distributions into the wettability analysis program. The area under each distribution was then normalized to one saturation unit. Figure 3 shows a typical stack plot for a  $S_{mix}$  spatial-T<sub>2</sub> distribution along with an intensity plot (Figure 3-inset) generated from the same data. The data plotted in Figure 3 is the corresponding spatial-T<sub>2</sub> data taken from the same sample as the bulk data plotted in Figure 1 and 2.
2. Perform a least-squares fit, minimizing the difference between  $S_{mix}$  (slice 1) –  $S_{pred}$  using Equation 5 to generate  $S_{pred}$  where  $S_{w-100\%}$  and  $S_{o-100\%}$  are now from the first slice of their spatial-T<sub>2</sub> distributions. The least squares fit will result in H and W functions for slice 1.
3. Employ the H and W functions to calculate  $I_{wett}$  and  $S_{wett}$  for slice 1.

This procedure is repeated until each slice of the spatial-T<sub>2</sub> distributions has been analyzed and  $I_{wett}$  and  $S_{wett}$  as a function of position in the rock have been created. It should be noted that the wettability and saturation derived from  $S_{mix}$  bulk data is used as an initial guess for each slice in the spatial-T<sub>2</sub> analysis. Also, to ensure that the spatial wettability and saturation derived

are free of discontinuities, the least square fit of each slice is restricted to not vary substantially from the results of the previous slice.

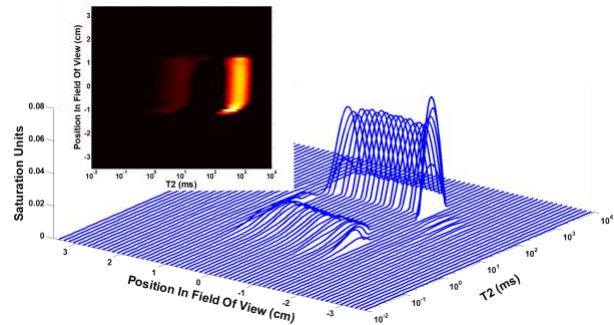


**Fig. 3:** Spatial-T<sub>2</sub> spectra for the same sample as the bulk spectra in Figure 1. The inset shows the intensity plot generated from the spatial-T<sub>2</sub> data.

## 4 Results

Figure 4 shows the spatial-T<sub>2</sub> wettability analysis completed on sample 109S. The upper plots show the spatially dependent wettability (blue traces) and saturation (red traces) profiles derived for each centrifuge speed tested. The rocks began at 100% brine saturated and had dodecane spun into them from left to right on the upper plots of Figure 4. Also shown in the upper panels of Figure 4 are the saturation profiles (black traces) derived from separate measurements where the rock was initially saturated to 100% with D<sub>2</sub>O rather than H<sub>2</sub>O before having dodecane spun into them. Employing NMR invisible D<sub>2</sub>O allowed the saturation profiles to be derived directly from the NMR data. It should also be noted that because D<sub>2</sub>O is denser than H<sub>2</sub>O, the centrifuge speeds were reduced to match the capillary pressures employed with H<sub>2</sub>O. These D<sub>2</sub>O profiles were then used to independently verify the accuracy of the profiles derived from the wettability fitting. There is no similar method for verifying the wettability as a function of position. The lower panels of Figure 4 show the intensity plots created from the spatial-T<sub>2</sub> data for the mixed saturation samples tested at each centrifuge speed.

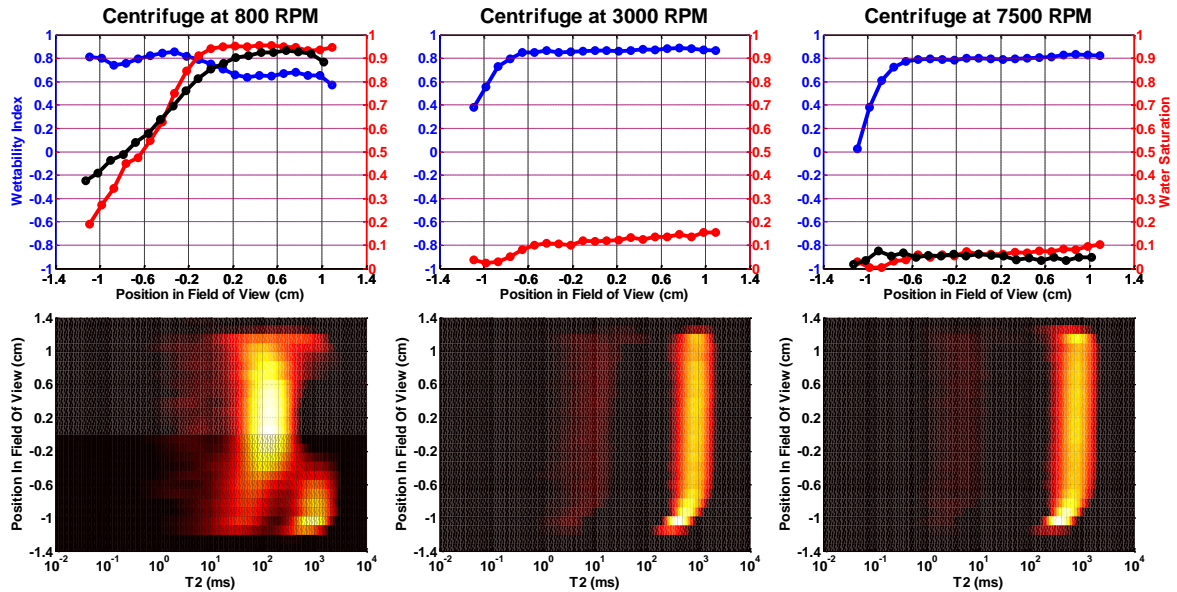


**Fig. 4.** The predicted wettability (blue) and saturation (red) profiles for rock 109S are plotted in the upper panels. The lower panels show the intensity plots generated from the spatial-T<sub>2</sub> data from the mixed saturation samples.

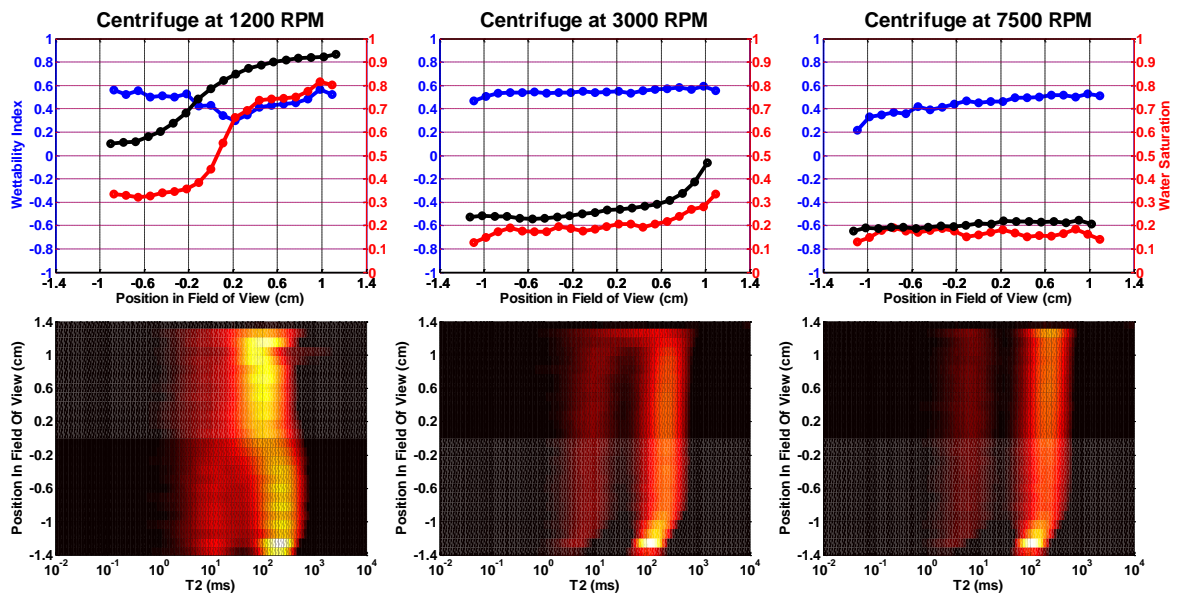


**Fig. 5.** The predicted wettability (blue) and saturation (red) profiles for rock 62A are plotted in the upper panels. The lower panels show the intensity plots generated from the spatial-T<sub>2</sub> data from the mixed saturation samples.

For 800 RPM, the saturation profile derived from wettability fitting agrees well with that measured using D<sub>2</sub>O. There is clearly a saturation gradient along the length of the rock. The average saturation for the rock is 0.71. The wettability on the other hand does not show the same variability with position. It is relatively constant across the rock independent of both position and water saturation. The average wettability across the rock is 0.73 making the rock water wet. For 3000 RPM, the saturation across the rock is now relatively uniform and significantly reduced as compared to 800 RPM. The average saturation is now 0.11 and the average wettability is now 0.82. D<sub>2</sub>O data was not recorded at 3000 RPM so there is no comparison between the predicted and measured

saturation profiles. For 7500 RPM, the saturation and wettability are again uniform along the rock. The average saturation is now 0.06 and the saturation profile agrees well with the corresponding D<sub>2</sub>O saturation profile. The average wettability is now 0.73. Both the saturation and wettability have decreased only slightly as compared to 3000 RPM.

Figure 5 shows the wettability (blue traces) and saturation (red traces) spatial data derived from the wettability fitting along with the intensity plots derived from the spatial-T<sub>2</sub> data for sample 62A. Again, the saturation profiles (black traces) derived from separate measurements where the rock was initially saturated to 100% with D<sub>2</sub>O rather than H<sub>2</sub>O are shown. Unlike for

rock 109S, there is not as good agreement between the predicted saturation profile and the D<sub>2</sub>O measured profile at each centrifuge speed. For example, at 800 RPM, the average saturation derived from the wettability fitting (red trace) is 0.55 whereas the average saturation derived from the D<sub>2</sub>O data is 0.77 (black trace). While this corresponds to an over 20% difference in measured versus predicted saturations, the overall shape of the saturation profiles is similar meaning the relative changes in saturation predicted from the wettability fitting are good. The difference between the predicted and measured saturations improves as the centrifuge speed increases and the water saturation decreases. For 3000 RPM, the predicted saturation is 0.20 whereas the average saturation from the D<sub>2</sub>O data is 0.28. For 7500 RPM, the predicted saturation is 0.17 whereas the average saturation from the D<sub>2</sub>O data is 0.20. The reason for the improvement is that as the centrifuge speed increases the T<sub>2</sub> spectra become less complex because two peaks (one for dodecane and one for brine) begin to separate. This separation of the peaks leads to an improved quality of the least-squares fit and hence a better prediction of the saturation in rock. Despite the inaccuracy of predicting the saturation of the rock as a function of position, the wettability predicted is unaffected. For each centrifuge speed the wettability is found to be water wet and relatively uniform across the rock.

Figure 6 shows the wettability (blue traces) and saturation (red traces) spatial data derived from the wettability fitting along with the intensity plots derived from the spatial-T<sub>2</sub> data for sample 96S. Again, the saturation profiles (black traces) derived from separate measurements where the rock was initially saturated to 100% with D<sub>2</sub>O rather than H<sub>2</sub>O are shown. For 700 RPM, the wettability fitting was not good. Clearly there

is not good agreement between the predicted saturation profile (red trace) and the measured saturation profile (black trace). In addition, the wettability fluctuates from one end of the rock to the other. This 700 RPM data is clearly a case where the wettability fitting is a failure due to the complex T<sub>2</sub> spectra of the mixed wettability sample. Luckily, the spectra for 3000 RPM and 7500 RPM where not as complex and accurate saturation and wettability profiles were derived from this data (Figure 6 – center and rightmost panels). For 3000 RPM, the average saturation predicted from the wettability fitting is 0.08 and there is no D<sub>2</sub>O data for comparison. For 7500 RPM, the average saturation predicted from the wettability fitting is 0.09 which compares well with the average saturation of 0.05 measured from the D<sub>2</sub>O data. The wettabilities predicted at both 3000 RPM and 7500 RPM indicate that the rock is slightly water wet.

While no other technique exists for measuring wettability as a function of position, the average wettability derived from the spatial-T<sub>2</sub> data can be compared with wettability determined from other methods such as the Fleury NMR method [1] and an Amott test. These comparisons were completed for samples 109S and 96S and the results are summarized in Table 3. For the sake of this comparison, the 7500 RPM data was used. While there is no reason to think the absolute value for the wettabilities derived from each method summarized in Table 3 should be equal, there should still be consistency in the wettability predicted for each rock. This is true for the data summarized in Table 3 where each method indicates that each rock is water wet. These results are consistent with other studies [6,7,11] which have showed that the Looyestijn NMR wettability index is consistent with the Amott wettability.

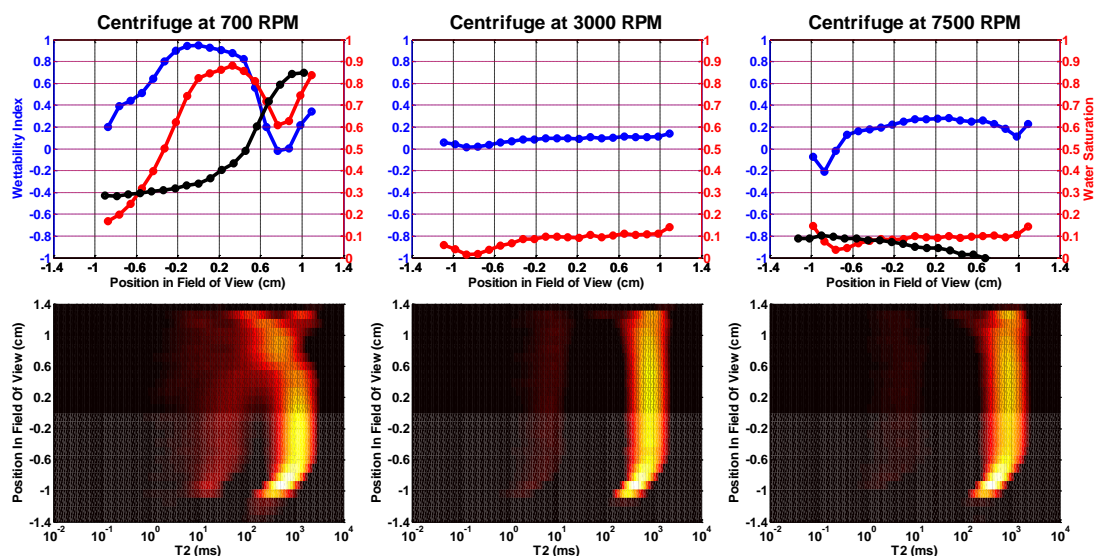


**Fig. 6.** The predicted wettability (blue) and saturation (red) profiles for rock 96S are plotted in the upper panels. The lower panels show the intensity plots generated from the spatial-T<sub>2</sub> data from the mixed saturation samples.

**Table 3:** Wettability Comparisons

Sample	Wettability – Looyestijn Method (This work 7500 RPM)	Wettability- Fleury Method	Wettability- Amott Method
96S	0.17	0.37	0.22
109S	0.73	0.43	0.21

## Conclusion

A new method for determining the wettability as a function of position in a core sample has been presented. This method couples the wettability determination via NMR  $T_2$  distributions method [6,7] with spatial- $T_2$  data. Using this method, we have successfully determined the wettability as a function of position for three sandstone samples with mixed saturations. The mixed saturation samples were created via centrifugation of dodecane into initially 100% water saturated samples. In each case, the wettability was found to be relatively uniform across the rock. Each rock on average was found to be water wet which is consistent with wettabilities determined for these samples via the Fleury method [1] and an Amott test. In addition to determining the wettability as a function of position, the spatial- $T_2$  wettability method presented here also predicts saturation as a function of position in a core sample. The accuracy of this saturation prediction was tested in this work using the same mixed saturation samples used for testing the wettability as a function of position. The accuracy of the saturation profiles were confirmed using saturation profiles determined from separate measurements where the same rock samples were initially saturated to 100% with  $D_2O$  rather than  $H_2O$ . Employing NMR invisible  $D_2O$  allowed the saturation profiles to be derived directly from the NMR data. The saturation profiles derived via NMR didn't always agree absolutely with the saturation profiles measured with  $D_2O$ . The difference in the predicted and measured saturation values could be as much as 20%. However, the relative saturation values within one predicted saturation profile always agreed well with the measured profile. Also, the quality of the least-squares fit improved and the accuracy of the saturation predicted got better if the  $T_2$  spectrum contained less complexity and overlapping of oil and water peaks. Finally, the wettability showed little change correlated to saturation level of the rock.

Based on our work, we have devised a procedure to derive the wettability (both bulk and spatial) of samples via NMR.

1. Record  $T_2$  and spatial- $T_2$  spectra of the mixed saturation sample of interest (as received or saturated in the lab).
2. Clean and dry the sample. Saturate the sample to 100% with brine. Record the  $T_2$  and spatial- $T_2$  spectra of the 100% water saturated sample.
3. Clean and dry the sample. Saturate the sample to 100% with oil of interest. Record the  $T_2$  and spatial- $T_2$  spectra of the 100% oil saturated sample.
4. Record the  $T_2$  spectra of bulk brine and oil.

5. Apply the fitting methods outlined in this paper to derive wettability and saturation as function of position.

The work presented in this paper was limited to saturation with only brine and dodecane. To truly observe wettability changes, experiments should be completed with crude oil rather than dodecane. In addition, the aging process should be observed over extended periods of time at elevated pressure and temperature with crude oil. The centrifuge method with dodecane presented here may not achieve measurable wettability changes. As a result, we have yet to test the spatial wettability method on an oil wet rock. For future work, we propose furthering our study by repeating our experiments with crude oil and adding observation of wettability changes over time with this crude oil.

## References

1. Fleury, M. and Deflandre, F., "Quantitative evaluation of porous media wettability using NMR relaxometry", *Magnetic Resonance Imaging* (2003), **21**, 385-387.
2. Howard, J.J., "Quantitative estimates of porous media wettability from proton NMR measurements", *Magnetic Resonance Imaging* (1998), **16**, 529-533.
3. Borgia, G. C., Fantazzini, P. and Mesini, E., "Wettability effects on oil-water configurations in porous media, a nuclear magnetic resonance relaxation study", *J. Appl. Phys.*, **70**, 7623-7625.
4. Hsu, W. F. and Flumerfelt, R. W., "Wettability of porous media by NMR relaxation methods", *SPE Annual Technical Conference and Exhibition*, Washington, D.C., USA, 4-7 October 1992.
5. Freedman, R., Heaton, N., Flaum, M., Hirasaki, G. J., Flaum, C. and Hurlimann, M., "Wettability, saturation and viscosity from NMR measurements", *SPEJ*, **8**, 317-327.
6. Looyestijn, W.J. and Hofman, J.P., "Wettability Index Determination by Nuclear Magnetic Resonance", SPE 93624, presented at the MEOS, Bahrain, March 2005. Published in *SPEREE* April 2006, pp 146 – 153.
7. Looyestijn, W., Zhang, X., and Hebing, A., "How can NMR assess the wettability of a chalk reservoir", *Society of Core Analysts*, Vienna, Austria, 27 August-1 September 2017.
8. JS-7.5 Swinging Bucket Rotor User Manual, J-TB-007AR, Beckman Coulter.
9. Geo-Spec 2-75 User Manual, Version 1.8, Oxford Instruments.
10. GIT Systems and LithoMetrix User Manual, Revision 1.9, Green Imaging Technologies.

11. Al-Muthana, A.S., Hursan, G. G., Ma, S. M., Valori, A., Nicot, B., Singer P. M., “Wettability as a function of pore size by NMR”, Society of Core Analysts, Aberdeen, Scotland, 27-30 August 2012.